

DETECTING DEFECTS in REINFORCED CONCRETE USING the METHOD of INFRARED THERMOGRAPHY

Bojan **Milovanović**, UNIVERSITY OF ZAGREB, FACULTY OF CIVIL ENGINEERING, Zagreb, HRVATSKA, Contact – +385 1 4639 316; bmilovanovic@grad.hr

Ivana **Banjad Pečur**, UNIVERSITY OF ZAGREB, FACULTY OF CIVIL ENGINEERING, Zagreb, HRVATSKA, Contact – +385 1 4639 162; banjadi@grad.hr

ABSTRACT – This paper presents a method for detecting defects in reinforced concrete structures by using the method of active infrared (IR) thermography. Non-destructive testing using infrared (IR) thermography consists of thermal stimulation of the object of interest and monitoring of the surface temperature variation during the transient cooling or heating process. The paper includes short descriptions of the post-processing methods used for detection of defects, together with the results of the research conducted on reinforced concrete samples. It was concluded that the method of IR thermography can be used for the detection and quantification of defects in reinforced concrete structures.

Keywords: non-destructive testing, IR thermography, reinforced concrete, step heating thermography

1. INTRODUCTION

Durability of reinforced concrete structures is a serious problem throughout the world, and thus assessment of the condition of concrete structures in order to determine the remaining service life and the method of repair is becoming increasingly important. In developed countries, the costs of repairs exceed the cost of building new structures.

The objective of condition assessment of existing reinforced concrete structures is to provide insight into current condition of the observed structure, to predict development of deterioration, and to assess the influence of defects found on the safety and life expectancy of the structure. During the condition assessment of reinforced concrete structures it is necessary to implement reliable and effective non-destructive testing methods which can detect, localize and characterize different types of defects. The advantage of non-destructive methods is their simplicity and the fact that they do not damage the structure or cause only minor surface damage. Interpretation of the results, however, is one of the most challenging tasks in modern construction process.

Although infrared (IR) thermography is being used in civil engineering for identification of heat losses through the building's thermal envelope, it has been realized its potential as one of the non-destructive thermal methods for nondestructive testing of materials and structures [1-3]. Nondestructive testing using IR thermography generally consists of thermal stimulation of the object under examination and monitoring of its surface temperature variation during the transient heating or cooling phase. The existence of inhomogeneities in the core material affects the heat transfer and thus causes local changes of temperature distribution on the surface of the observed structure, which is then recorded using an IR camera [4].

Defects like voids in concrete or masonry or delaminations at interfaces of composites which have different density, heat capacity and/or heat conductivity in comparison to the bulk material can be localized and characterized.

In this paper, experimental investigations on concrete test specimen containing voids with different sizes and depths were analyzed.

2. EXPERIMENTAL WORK

A literature review was used to analyze approach of individual researchers to using IR thermography for defects determination in concrete structures. Based on the results found, specimen and defect size, together with thermal excitation used by the researchers, specimens used in presented paper were determined. Specific specimen size was defined by the need that there is a possibility of transferring specimens (limited by the dimensions and weights of the samples) and conditioning of the specimens in the curing chamber, while on the other hand, samples needed to be large enough to be able to simulate real defects, without the influence of specimen edges or the influence of defects between themselves on the temperature field.

The effect of reinforcement spacing on the possibility of detection defects deeper than the thickness of the concrete protective layer. Influences of concrete properties (density and moisture content) which indirectly influence on the thermal properties of the concrete possibility to carry out measurements were also investigated.

The research was conducted by using reflecting method of testing, where surface temperature was monitored during thermal excitation (duration of 60 minutes), together with the cooling period lasting also 60 minutes, **Figure 1**, **Figure 2**. Thermal excitation was performed using halogen lamp with the power of 1000 W, with the heating distance of 1.5; 2.0 and 3.0 m from the surface of concrete samples.

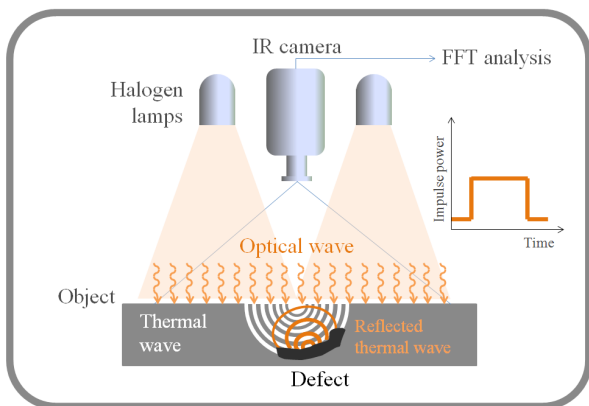


Figure 1 Schematic representation of the reflective method of testing



Figure 2 Experimental setup of the thermal excitation, heating distance of 1.5 m from the specimen surface

A schematic drawing and photographs of the concrete test specimen with voids are shown in **Figure 3** and **Figure 4**, respectively. For simulating compaction defects and voids made of polystyrene foam have been incorporated. These defects vary in size (discs of 15 cm in diameter and rhombus 17×12.6 cm both with thickness of 4 cm). In the specimen, one of the discs is positioned underneath the reinforcement with the rebar spacing of 50 mm, while the other disc is positioned under the reinforcement with the rebar spacing of 100 mm, while rebar diameter is 8 mm. Additionally, rhombus is placed both under the 50 and 100 mm reinforcement. Depth of all defects is 30 mm from both sides of the specimen. It is important to emphasize that the specimens were tested from both sides, where the reinforcement was placed only from one side, while the other side of the specimen didn't have any reinforcement between the defects and the surface.

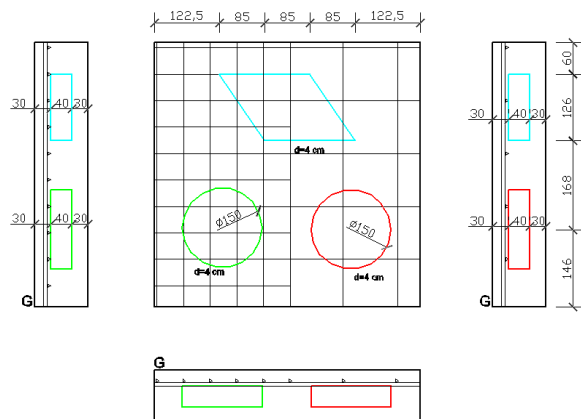


Figure 3 Schematics of the concrete test specimen with polystyrene defects



Figure 4 Concrete test specimen with polystyrene defects, preparation stage and finished specimen

For pre and post-processing of test results algorithms and programs (known as M-files) in MATLAB code have been developed, which were used for each step of results analysis.

The technique used in the post-processing of test results, or the detection of defects is known as the pulse phase thermography (PPT), where phase and amplitude images were considered.

To carry out measurements in this study, an IrNDT system, manufactured by Automation Technology GmbH was used, which enables the use of the step heating and lock-in techniques together with pulsed thermography technique for NDT of samples where halogen lamp is being used as the thermal excitation source. This instrumentation allows the study of the impact of the magnitude and phase of heat waves on the specimens at hand, and it is necessary to accurately monitor the time dependence between the output signal and the reference signal input. To carry out the measurements, infrared camera FLIR ThermaCAM P640 was used with the properties as shown below, **Table 1**.

Table 1 Technical specifications of FLIR P640 camera

IR camera characteristics	
Spectral range	7.5 - 13 μm
IR resolution	640x480 pixel
Field of view (FOV)	24°x18°
Minimum focus distance	0.3 m
Spatial resolution (IFOV)	0.65 mrad for 24° lens
Thermal sensitivity (NETD)	60 mK @ 30°C
Image frequency	30 Hz
Accuracy	± 2 °C or $\pm 2\%$ of reading
Temperature range	-40°C to +120°C
	0°C to +500°C
	300°C to 2000°C

FLIR P640 IR camera operates in long-wave (LWIR) spectral range (7,5 – 13 μm). Detector used is so called uncooled microbolometer, which is in fact focal plane array (FPA) detector composed of 307200 (640x480) individual detectors. Bolometers are generally very sensitive resistance thermometers which alter their electrical resistance when exposed to the change of temperature.

The camera is connected to the computer and the thermal excitation system using the active thermography electronic interface.

As thermal excitation 1000 Watt halogen lamp (Parabolic aluminized reflector - PAR reflector) was used, which is suitable for homogeneous heating of the surface area up to 1 m². Halogen lamp is controlled electronically via a computer program and over IRX-Box, which modulates its operation with the recording sequence of the IR camera.

3. METHODS

Pulse phase thermography (PPT) is active infrared technique which enables the collected data to be transformed from the time domain to the frequency domain using a one-dimensional discrete Fourier transform (DFT) [6,7].

PPT is well known for non-destructive testing of materials and structures. It combines features of pulse thermography (PT) and lock-in thermography (LT) techniques and thus enables an easy data acquisition and automatic and fast data analysis.

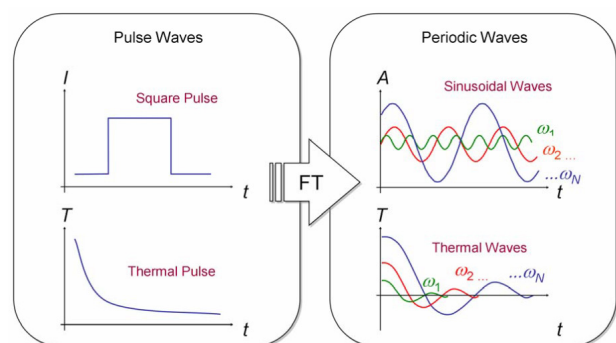


Figure 5 Experimental configuration PT vs LT [8]

Although not evident at first sight, a link between PT and LT can be established through the superposition principle. It is well-known that any wave form, periodic or not, can be approximated by the sum of purely harmonic waves oscillating at different frequencies [8], **Figure 5**.

The pulsed forms on the left side (square and thermal decay) (**Figure 5**) can be approximated by a sum of sinusoids (only three harmonics are included for simplicity) with frequencies ranging from 0 to ∞ .

In practice, actual frequencies (minimum, maximum), as well as frequency resolution, depend on equipment limitations as well as on sampling and truncation parameters. Hence, it is possible to extract a certain number of thermal waves from a thermal pulse, each one having a different frequency, amplitude and phase delay, though a transformation algorithm such as the Fourier Transform [8].

In PPT, thermal data is processed with the Fourier Transform (FT), Eq. (1):

$$F_n = \Delta t \sum_{k=0}^{N-1} T(k\Delta t) e^{\left(\frac{-j2\pi nk}{N}\right)} = Re_n + Im_n \quad (1)$$

where “j” denotes imaginary unit ($j^2=-1$), “n” designates the frequency increment, “ Δt ” is the sampling interval, and “Re” and “Im” are the real and the imaginary parts of the transform, respectively. Real and the imaginary parts of the transform are being used for calculating the amplitude “A”, Eq. (2), and the phase delay “ \varnothing ”, Eq. (3), of the transform.

$$A_n = \sqrt{Re_n^2 + Im_n^2} \quad (2)$$

$$\varnothing_n = \tan^{-1} \left(\frac{Im_n}{Re_n} \right) \quad (3)$$

Reconstruction of the 3D matrix can be performed as illustrated in **Figure 6**.

Matrices illustrated in **Figure 6** are obtained by applying equations for “A_n” and “ \varnothing_n ” on every pixel of the thermogram sequence.

Temperature profiles, obtained by measuring the temperature evolution during cooling cycle for one pixel are real functions

that produce a transform with an even (or symmetrical) real part and an odd (or anti-symmetrical) imaginary part. This kind of function is referred as Hermite function and as seen in **Figure 6**, the symmetry properties of a Hermite function are reflected on the amplitude and phase of the transform, which are even and odd, correspondingly, with respect to $f=0$ Hz (i.e. $n=N/2$). Therefore, from a sequence of N thermograms, there are N/2 useful frequency components; the other half of the spectra only provides redundant information. Negative frequency data can thus be safely discarded [8].

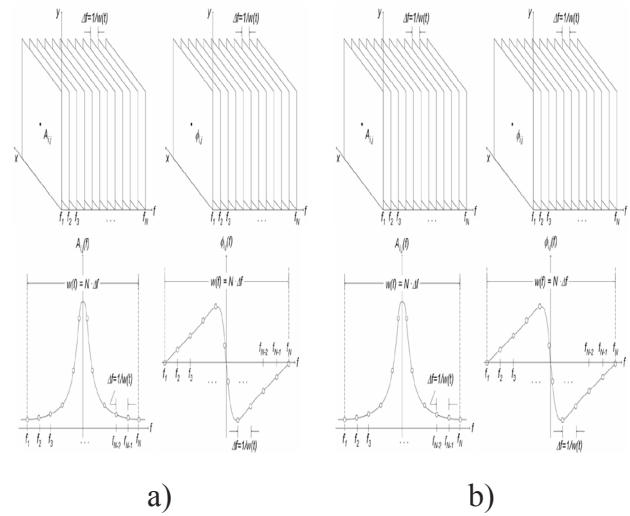


Figure 6 (a) Amplitude; and (b) phase sequences (top) and their corresponding profiles on the frequency spectra for a non-defective pixel on coordinates (i,j) (bottom) [8]

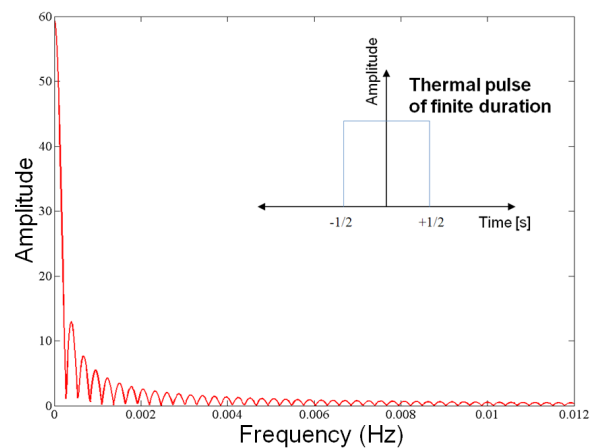


Figure 7 Amplitude [dB] of long-lasting rectangular thermal pulse in frequency domain

Figure 7 shows the real part of the corresponding frequency spectrum for the pulse of a given duration, and displays the amplitude of long-lasting rectangular

thermal pulse for the specimen with the thermal excitation at a distance of 1.5 m, obtained after executing the fast Fourier transform on the temperature development curves of the specimen surface above the sound area.

Thermal pulses of longer duration in the time domain have a narrower spectrum in the frequency domain, while the available energy is concentrated in the lower frequencies hence the lower frequencies penetrate deeper into the specimen [7].

Discrete frequencies “ f_n ” for which phase delay (phasegrams) and amplitude (ampligrams) images can be reconstructed are given with the following equation, (4) [7]:

$$f_n = \frac{n}{N\Delta} \quad (4)$$

The maximum frequency is limited by the sampling rate of the thermograms; and therefore with the characteristics of the equipment used, in particular with the camera characteristics, while the minimum frequency is determined by the duration of the experiment, i.e. number of thermograms in the sequence.

In practice, it is possible to use only the first few frequencies for depicting and detection of the defects, because of the fact that the largest part of the energy is concentrated in the low frequencies, while higher frequencies show higher noise level which prevents the possibility of defect detection [7].

4. RESULTS

4.1. PPT – PHASEGRAMS

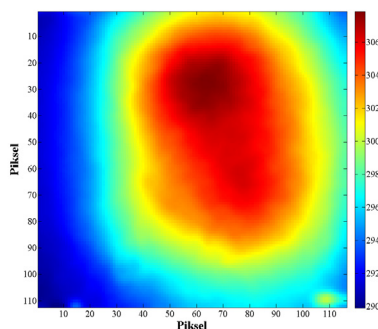


Figure 8 Thermogram – thermal excitation distance 1.5m

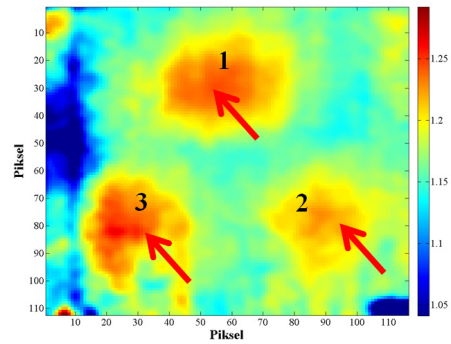


Figure 9 Phasegram $f=5,540 \times 10^{-4}$ Hz – thermal excitation distance 1.5m

In this chapter the results of the pulse phased thermography technique in the form of phasegrams are presented, all given with their specific discrete frequencies f_n obtained from the analysis of the principal components. These discrete frequencies are characteristic for individual samples and for the entire set of test results.

Figure 8 and **Figure 9** show an example of comparison of test results, optimal thermogram and with post-processing using FFT analysis ($f = 5.540 \times 10^{-4}$ Hz), respectively, where thermal excitation was at the distance of 1.5 m from the specimen surface. The figures show a noticeable improvement in the possibility of detecting damage in case of using the phasegram compared to thermogram.

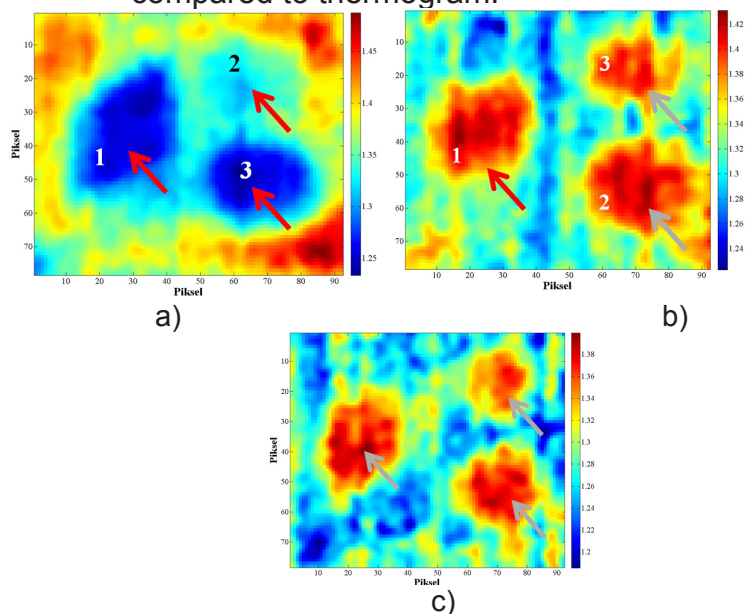


Figure 10 Phasegram – thermal excitation distance 1.5m: a) $f=4,751 \times 10^{-4}$ Hz
 $f = 4,751 \times 10^{-4}$ Hz; b) $f=1,188 \times 10^{-3}$ Hz
 $f = 1,188 \times 10^{-3}$ Hz; c) $f = 2,850 \times 10^{-3}$ Hz
 $f=2,850 \times 10^{-3}$ Hz

Figure 10 shows the possibility of detecting defects in the specimens when the thermal excitation is at the distance of 3 m from the surface of the specimen, all in dependence of the specific discrete frequency of phasegrams. It can be seen that depending on the discrete frequency, the extreme used for detecting defects is changing from minimum to maximum. Additionally, it can be concluded that optimal discrete frequency exists, which enables the best possible contrast between sound area and defects, and at which the noise is minimal. With the further increasing of the discrete frequency, noise is being increased while the contrast between the damaged and sound areas of the sample is being reduced to the point when it is no longer possible to detect any defects, **Figure 11**. This leads to the conclusion that if phasegram for one discrete frequency is being regarded, without the context of phasegrams for all other frequencies, it is possible to overlook the existence of certain or all defects.

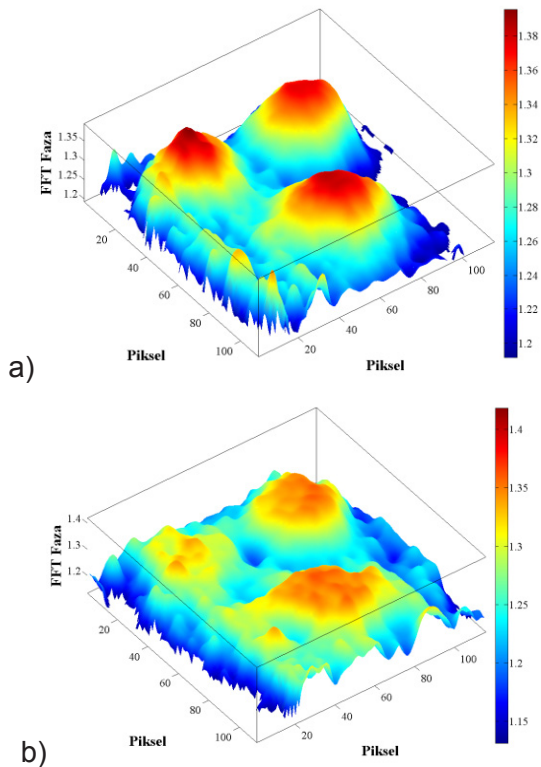


Figure 11 Phasegram – thermal excitation distance 1.5m: a) $f=1,096 \times 10^{-3}$ Hz; b) $f=3,562 \times 10^{-3}$ Hz

Figure 12 gives a comparison between phasegrams for the specimen heated from the bottom side where there is no

reinforcement between the defects and the specimen surface and the upper side of the specimen where reinforcement exist between the defects and the specimen surface, all according to the schematics presented in **Figure 3**.

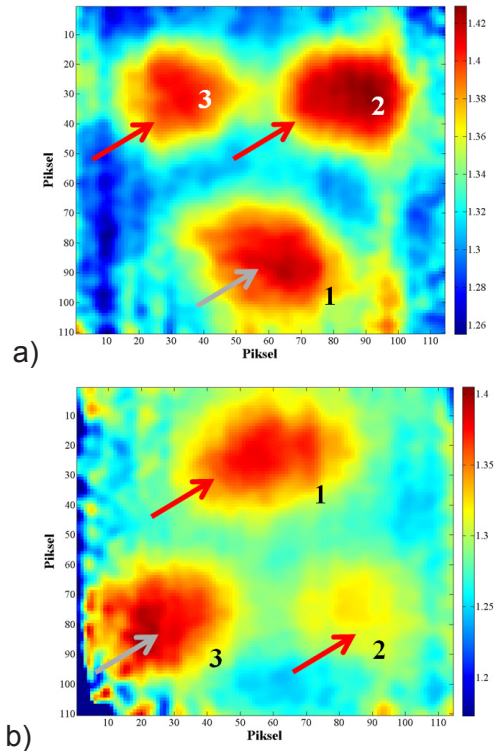


Figure 12 Phasegram – thermal excitation distance 1.5m, a) without reinforcement, $f=1,301 \times 10^{-3}$ Hz; b) with reinforcement $f=1,370 \times 10^{-3}$ Hz

From the presented, it is evident that the existence of reinforcement affects the possibility of detecting damage and its characterization (size and shape), where for the defect No. 2 viewed from the upper side (defect under dense reinforcement), the contrast between the defect itself and the sound area is very small thus decreasing its detection possibility.

4.2. PPT – AMPLIGRAMS

This chapter gives an overview of the test results, the possibilities and limitations of using pulse phased thermography (PPT), and methods of post-processing of test results by using the fast Fourier transform i.e. the amplitude images (ampligrams) in the results analysis.

The presented results are given for the

sequence of thermograms taken during the cooling period of the specimens that were previously heated using 1000W halogen lamp as thermal excitation for 60 minutes.

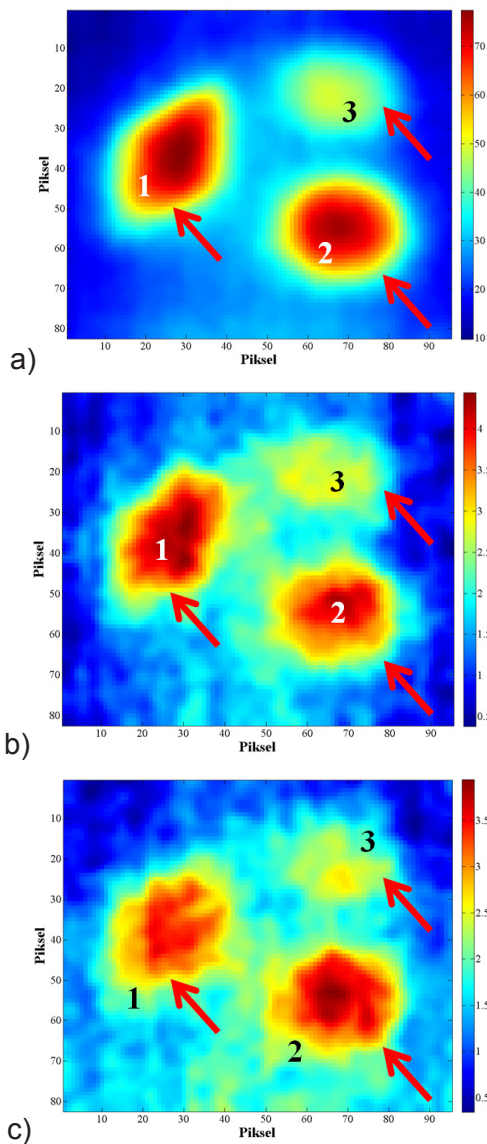


Figure 13 Ampligrams – thermal excitation distance 2 m; a) $f=1,671 \times 10^{-3}$ Hz; b) $f=27,855 \times 10^{-3}$ Hz; c) $f=55,710 \times 10^{-3}$ Hz

As already shown in the case of phasegrams, the following figures show the results in the form of amplitude images (ampligrams) for the specific discrete frequencies f_n obtained from the analysis of the principal components, which are characteristic frequencies of individual samples and for the entire set of test results.

Figure 13 gives the ampligrams depending on the discrete frequency gained after performing an FFT analysis of the sequence

of thermograms sampled during the cooling of the specimen which was thermally excited from a distance of 2 m from the specimen surface. Herein, it is necessary to emphasize the difference in the possibility of detection and characterization of damage depending on the specific discrete frequency in question. At lower frequencies, it is possible to determine the shape of the damage, because of the reduced noise and better contrast between the defect and sound areas of the specimen.

If thermogram sequence is captured after the heating period of concrete and ampligrams are used for the detection of defects, it is possible to detect the defects that are no longer visible on thermograms, enhancing the reliability of the presented technique, **Figure 14**.

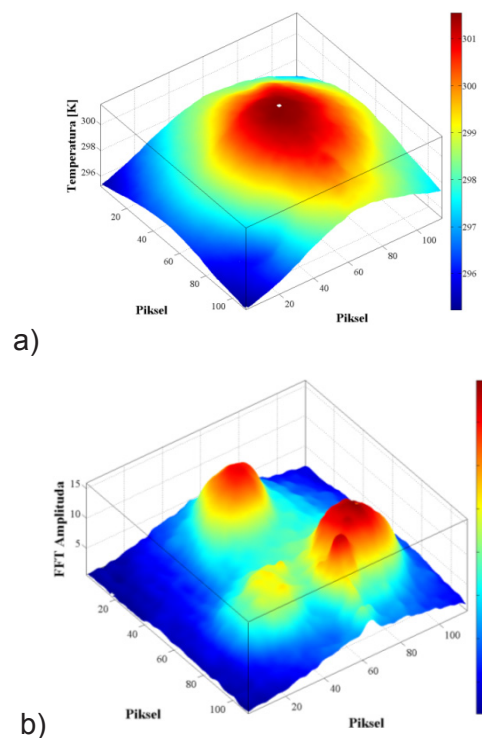


Figure 14 Thermal excitation distance 3 m; a) Thermogram taken 42,67 min after the shutdown of thermal excitation; b) Ampligram, $f=67,368 \times 10^{-3}$ Hz

Application of ampligrams as the methods used to display the testing results acquired by active thermography does not solve the problem of uneven heating of the samples, but only reduces its impact, **Figure 15**.

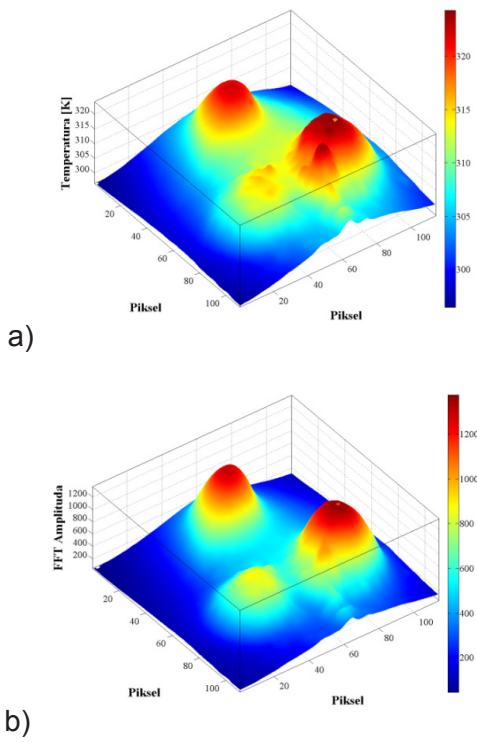


Figure 15 Thermal excitation distance 3 m; a) Optimal thermogram; b) Ampligram, $f=5,263 \times 10^{-4}$ Hz

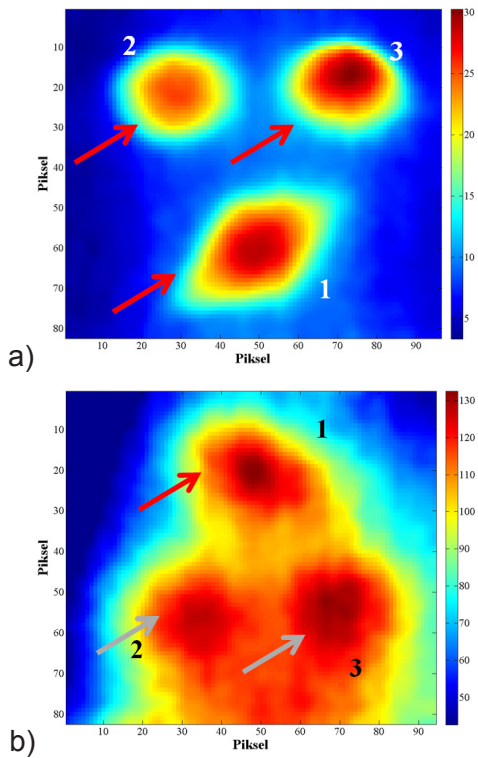


Figure 16 Ampligrams - thermal excitation distance 2 m, a) $f=5,785 \times 10^{-3}$ Hz; b) $f=5,050 \times 10^{-4}$ Hz

It is particularly important to emphasize the possibility of misinterpretation of test results if ampligrams are being used, due to their inability to eliminate reflections, making it possible to come to a false positive

test results, **Figure 15**. In the **Figure 15** reflections that emerged and which cannot be avoided in ampligrams are marked with an arrow.

Figure 16 gives the comparison of ampligrams of the sample without and with the reinforcement between the defects and specimen surface, respectively. Reinforcement significantly influences the testing results when ampligrams are analyzed; reinforcement significantly reduces the contrast between areas with defects and sound area of the specimens. This is particularly visible when defect No.2 is regarded, which is placed under the more dense rebar spacing.

Example in **Figure 16** is illustrative example of the effect of lateral diffusion of heat through the specimen, which then masks the existence of defects in the specimen itself. It has to be noted that defects are equidistant from both surfaces of the tested specimen, and the defect depth is 30 mm.

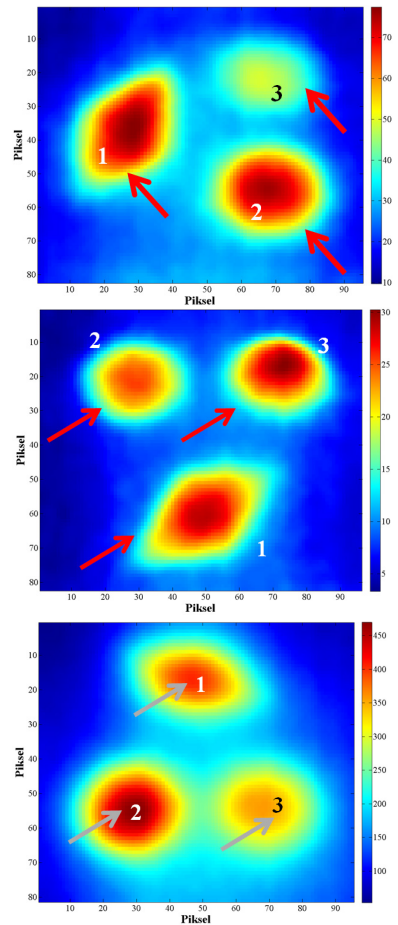


Figure 17 Ampligrams - thermal excitation distance 2 m, concrete compressive strength: a) 19 MPa ($f=1,671 \times 10^{-3}$ Hz); b) 41 MPa ($f=5,785 \times 10^{-3}$ Hz); c) 89 MPa ($f=5,764 \times 10^{-4}$ Hz)

Dependences of the ampligrams on the concrete quality is difficult to describe, since there is always a possibility to change slightly the discrete frequencies in order to gain the optimum ampligram regarding the possibility of defect detection for concrete quality at hand. **Figure 17** gives ampligrams for concrete with compressive strength of 19 MPa, 41 MPa and 89 MPa, respectively.

4.3. COMPLETE SEQUENCE – HEATING AND COOLING

If heating and the cooling process of the specimen are captured in one sequence, **Figure 18**, instead of analyzing only the cooling sequence, and if one carries out post processing of test results using FFT in the manner that have been previously described, it is possible to obtain the following results.

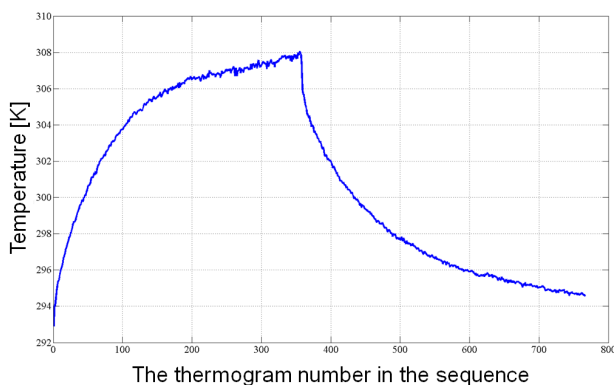


Figure 18 Temperature development on the surface of concrete sample throughout the heating and cooling period

In contrast to the results obtained solely from the cooling sequence, the phasegram image obtained from the complete sequence (heating and cooling process) using FFT analysis, only a few useful discrete frequencies (three to five frequencies) can be extracted. It has to be noted here that in the case of the phasegrams of the complete sequence defects have the opposite extreme than it was the case when phasegrams for the cooling sequence were analyzed, **Figure 19**.

When analyzing the ampligrams obtained executing FFT analysis of the complete sequence of thermograms (heating and

cooling) it was noted that only every other ampligram useful for determining the presence of defects in specimens. Similar to the phasegrams, ampligrams obtained from the complete sequence, give only a few useful discrete frequencies. Additionally, it was found that in the case of detecting small defects in the concrete specimens, contrast of the defects compared to the sound part of the specimen, better conditions for defect detection can be obtained in the case of using only the cooling sequence in the analysis.

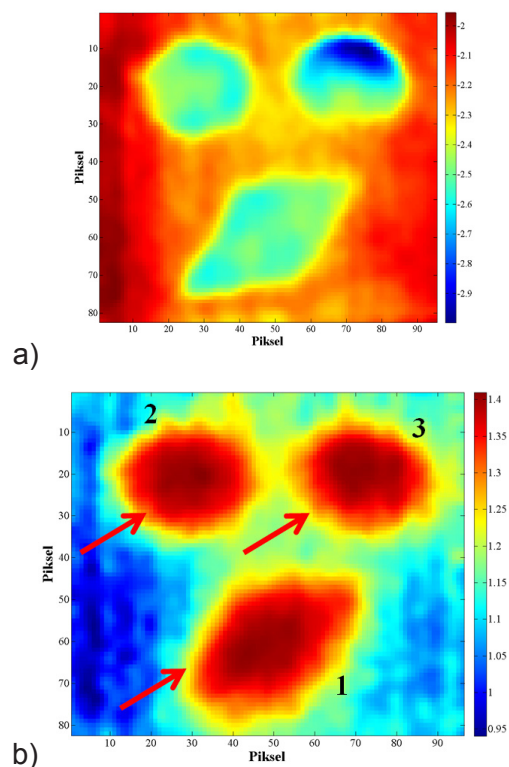


Figure 19 Thermal excitation distance 2 m: a) Phasegram, complete sequence, $f=8,333 \times 10^{-4}$ Hz; b) Phasegram, cooling sequence, $f=2,479 \times 10^{-3}$ Hz

Generally, it is possible to conclude that in the case of analyzing the small diameter defects, analysis of the cooling sequences and post-processing of only the part of cooling sequence proved to be better methodology. In the case of large defects (larger than 10 cm in diameter) with a relatively small depth (up to 3 cm), it is possible to conclude that there is no difference between the possibility of detecting defects by observing the test results obtained by the post-processing of the entire sequence or only cooling sequences.

5. CONCLUSIONS

The purpose of this paper was to present active techniques of infrared thermography that could be used for detection of near-surface inhomogeneities and common subsurface defects in typical structural elements made of concrete.

Optimal thermograms obtained using reflective method of testing was presented, together with examples of test results processed using fast Fourier transformation and presented in form of phasegrams and ampligrams. Results presented in this paper, and the conclusions derived from them were obtained using step heating technique of thermal excitation of concrete specimens.

The analysis of phasegrams for certain discrete frequencies f_n , it was found that for each specimen and testing procedure there is an optimal discrete frequencies at which the phasegram depict the best contrast and lowest noise. After the optimal discrete frequency a further increase in frequency also increases the noise to the point at which it is no longer possible to discover the existence of defects. It can be said that using techniques presented in this paper, defects of the minimum diameter of 10 cm at the depth of 7 cm or less can be detected with high probability.

The phasegram image solves the problem of non-uniform heating of the specimen, and also the problem with the reflectivity which proved to be significant regardless of the high emissivity of concrete and appears on the thermograms. In phasegrams reflected objects have the opposite extreme from damage and the pattern is changing depending on the discrete frequency observed. Reflection is thus relatively easily identified in the case of phasegrams, while in the case of analyzing of higher frequencies reflection completely disappears.

Ampligrams give only a slight improvement in the possibility of defect detection in comparison to the optimal thermogram, additionally at lower frequencies; it is possible to determine the shape of the damage, with the decreased noise compared to the higher

frequencies which enables a better contrast between the defect and the sound areas of the specimen.

Using ampligrams as the method used to display the active thermography testing results does not solve the problem of uneven heating of the specimens, it only reduces its impact thus only slightly improving test results, thus proving themselves to be inferior compared to the phasegrams. It is particularly important to emphasize the possibility of misinterpretation of test results if ampligrams are being used, due to their inability to eliminate reflections, making it possible to come to a false positive test results. The geometrical configuration of the defects can be determined from phase as well as from amplitude images.

Finally, it can be concluded that the results obtained using the method of active IR thermography are such that the method of pulse phase thermography (PPT) for post-processing of thermogram sequences can be used to detect defects in reinforced concrete structures.

6. LITERATURE

- [1] Milovanović, B.: „Karakterizacija oštećenja u armiranom betonu korištenjem metode infracrvene termografije“, Građevinski fakultet, Sveučilišta u Zagrebu, doktorska disertacija, Zagreb, 2013. (in Croatian)
- [2] Meola, C.: “A new approach for estimation of defects detection with infrared thermography”, *Materials Letters*, 61(3), 747–750, 2007.
- [3] Milovanović, B., and Banjad Pečur, I. (2011). Determination of material homogeneity using infrared thermography. *Proceedings of the V Conferencia Panamericana de Ensayos No Destructivos Cancun*. Cancun, Mexico.
- [4] Maierhofer, C.: „Transient thermography for structural investigation of concrete and composites in the near surface region“, *Infrared Physics & Technology* 43 (3-5), 271-278, 2002.

- [5] Andrassy, M., Boras, I., and Švaić, S. (2008). Osnove termografije s primjenom (p. 172). Zagreb: Kigen. (in Croatian)
- [6] Ibarra-Castanedo, C., Genest, M., Servais, P., Maldague, X. P. V., & Bendada, A.: “Qualitative and quantitative assessment of aerospace structures by pulsed thermography”, *Nondestructive Testing and Evaluation*, 22(2-3), 199–215. (2007).

- [7] Maldague, X. P. V.: “Theory and Practice of Infrared Technology for Nondestructive Testing”, (K. Chang, Ed.) (p. 684). John Wiley & Sons, Inc., (2001).
- [8] Ibarra-Castanedo, C.: “Quantitative subsurface defect evaluation by pulsed phase thermography: depth retrieval with the phase”, *Universite Laval Quebec*, (2005).

AUTHORS wish to thank Croatian Ministry of Education, Science and Sport which is funding the scientific project “From Nano to Macro-structure of Concrete”, 082-0822161-2990, within which presented research was conducted.

EuroTehnika d.o.o.

Sveta Nedelja-Novaki, Industrijski odvojak 3
 Tel: +385 1 2404 356, Mob: 098 9811513, Fax: +385 1 2404 359
 e-mail: mskelin@eurotehnika.hr www.eurotehnika.hr

Oprema i pribor za nerazorna ispitivanja – Balteau, Kodak i Olympus



Kodak

INDUSTREX Products
DISTRIBUTOR



OLYMPUS

Your Vision, Our Future

